Structure and Dynamics in the Local Universe

CSIRO PUBLISHING

Publications of the Astronomical Society of Australia, 2004, **21**, 396–403 www.publish.csiro.au/journals/pasa

Large Scale Structure in the Local Universe — The 2MASS Galaxy Catalog

Thomas Jarrett[A]

[A] Infrared Processing and Analysis Center, MS 100-22, California Institute of Technology, Pasadena, CA 91125, USA. Email: jarrett@ipac.caltech.edu

Received 2004 May 3, accepted 2004 October 12

Abstract: Using twin ground-based telescopes, the Two-Micron All Sky Survey (2MASS) scanned both equatorial hemispheres, detecting more than 500 million stars and resolving more than 1.5 million galaxies in the near-infrared (1–2.2 μm) bands. The Extended Source Catalog (XSC) embodies both photometric and astrometric whole sky uniformity, revealing large scale structures in the local Universe and extending our view into the Milky Way's dust-obscured 'Zone of Avoidance'. The XSC represents a uniquely unbiased sample of nearby galaxies, particularly sensitive to the underlying, dominant, stellar mass component of galaxies. The basic properties of the XSC, including photometric sensitivity, source counts, and spatial distribution, are presented here. Finally, we employ a photometric redshift technique to add depth to the spatial maps, reconstructing the *cosmic web* of superclusters spanning the sky.

Keywords: general: galaxies — fundamental parameters: infrared — galaxies: clusters — surveys: astronomical

1 Introduction

Our understanding of the origin and evolution of the Universe has been fundamentally transformed with seminal redshift, distant supernovae, and cosmic microwave background surveys. The focus has shifted to the distribution and nature of dark matter and dark energy that drive the dynamics of the expanding cosmos. The study of the local Universe, including its peculiar motions and its clustering on scales exceeding 100 Mpc, is an essential ingredient in the connection between the origin of structure in the early Universe and the subsequent formation of galaxies and their evolution to the state we observe today. Key issues include the location and velocity distribution of galaxies, leading to the mass-to-light relationship between what is observed and what is influencing the mass density field.

Spurred on by the enormous success of the redshift surveys (e.g. Huchra et al. 1983), conducted some 20 years ago, pioneers such as John Huchra proposed to image the entire sky at near-infrared wavelengths to create an unbiased census of galaxies that would fuel the next generation of redshift surveys (e.g. 6dFGS; see Watson et al. 2001 and Jones et al. 2004) and help address these weighty issues. After much deliberation, what finally transpired some ten years ago now, is the Two-Micron All Sky Survey (2MASS). Many years of observations and hard work to detect and extract sources has produced a gap-free image atlas of the entire sky, and catalogues containing stars and galaxies. The literature is now populated with many influential papers that used 2MASS to address fundamental extragalactic issues, including luminosity functions (e.g. Cole et al. 2001; Kochanek et al. 2001; Bell et al. 2003), galaxy morphology (e.g. Jarrett et al. 2003), distance indicators (e.g. Karachentsev et al. 2002), angular correlation functions (e.g. Maller et al. 2003a), and the dipole of the local Universe (e.g. Maller et al. 2003b). The 2MASS view of the 'cosmic web' — the space distribution of galaxies in the local Universe — is the focus of this paper. Figure 1 is an attempt to encapsulate our present understanding of the large scale structure that embodies the local Universe. Figure 2 provides a locator key to the extragalactic sky.

2 Two-Micron All Sky Survey

2MASS is a ground-based, near-infrared survey of the whole sky. It began operations in the mid-1990s and completed observations in early 2001. The final source catalogs and image Atlas were released to the public in the northern Autumn of 2002 (Cutri et al. 2000). 2MASS is fundamentally an imaging survey, with detection and source characterisation derived from images that span the near-infrared windows: J (1.2 μm), H (1.6 μm), and K_s (2.2 μm). The images were acquired using an efficient drift scan and freeze-frame technique, painting the sky with $8.5' \times 6°$ tiles or 'scans' (Skrutskie et al. 1997), forming 23 separate images per tile per near-infrared band of size 512×1024 pixels with resampled $1''$ pixels. A total of 4121439 FITS images cover 4π steradians of the sky. These images, $8.5' \times 17'$ in angular size, are also known as 'coadds' since they are comprised of ∼6 optimally dithered samples per pixel. The effective beam or PSF FWHM is ∼2 to $3''$, depending on the atmospheric seeing, and is roughly the same for each band. The typical 1σ background noise is 21.4, 20.6, and 20.0 mag arcsec^{-2} for

 10.1071/AS04050 1323-3580/04/04396

Figure 1 Panoramic view of the entire near-infrared sky reveals the distribution of galaxies beyond the Milky Way. The image is derived from the 2MASS Extended Source Catalog (XSC) — more than 1.5 million galaxies — and the Point Source Catalog (PSC) — nearly 0.5 billion Milky Way stars. The galaxies are colour coded by 'redshift', photometrically deduced from the K-band (2.2 μm) or as given in the NASA Extragalactic Database (NED). Blue are the nearest sources ($z < 0.01$), green are at moderate distances ($0.01 < z < 0.04$), and red are the most distant sources that 2MASS resolves ($0.04 < z < 0.1$). The map is projected with an equal area Aitoff in the Galactic system (Milky Way at centre). A locator key is provided in Figure 2.

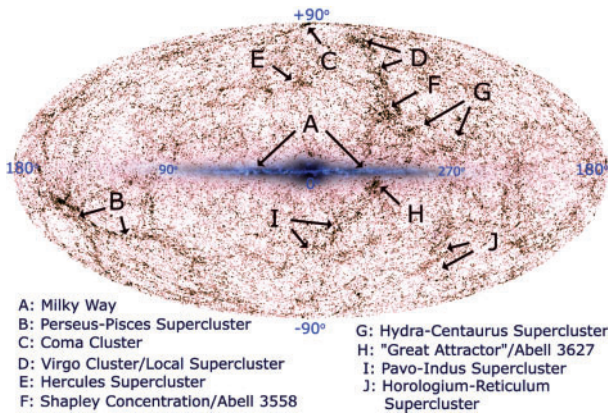

Figure 2 Galactic projection of the 2MASS Galaxy Catalog. Galaxy clusters and large scale structures, seen in Figure 1, are labelled here. The CMB dipole (Lineweaver et al. 1996) is located to the right of the Shapley Concentration (item 'F' in figure), while the galaxy clustering dipole (Maller et al. 2003b) is located 16° northward of the CMB dipole, adjacent to the Virgo and Shapley superclusters.

J, H, and K_s, respectively. The images include a photometric zero-point calibration that is accurate to 2–3% and an astrometric solution that is accurate to $<0.2''$ (Cutri et al. 2000).

Stars and galaxies are detected and characterised from the 2MASS images. The Point Source Catalog (PSC) contains ∼500 million objects, largely comprised of stars from the Milky Way. The Extended Source Catalog (XSC) contains ∼1.6 million objects clearly resolved by 2MASS, chiefly comprised of extragalactic sources in the local Universe. This paper will focus on these resolved galaxies. The images and source catalogs are available to the public through the Infrared Science Archive (IRSA) and NASA Extragalactic Database (NED) of IPAC.

3 The 2MASS Galaxy Catalog

The XSC contains over 1.6 million spatially resolved astronomical sources: primarily (>98%) galaxies, and to a lesser extent Galactic diffuse nebulae, HII regions, stellar clusters, planetary nebulae and young stellar objects. The *galaxy catalog* was constructed to satisfy the survey science requirements (Jarrett et al. 2000a), most important being the reliability (∼99%) and completeness (>90%) for unconfused regions of the sky, $|b| > 20°$. These requirements are achieved for sources brighter than $K_s = 13.5$ mag (∼2.7 mJy) and resolved diameters larger than ∼10–15 arcsec. The differential source counts, Figure 3, illustrate the depth and areal coverage of the 2MASS galaxy catalog for unobscured regions of the sky. The K_s-band counts increase linearly up to the faint-end limit, ∼14 mag, which are propped up by the more sensitive J-band observations, complete down to 15.3 mag.

3.1 Morphology

As a function of Hubble or morphological type, 2MASS is most sensitive to early-type spirals and ellipticals (whose light is dominated by the older population of stars emitting in the near-infrared), and less sensitive to late-type

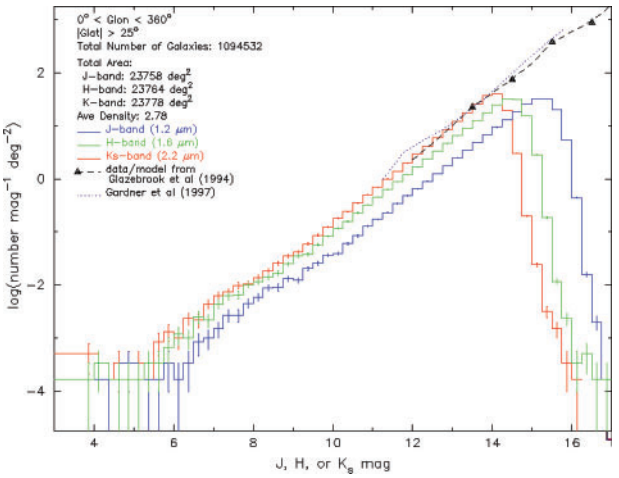

Figure 3 Total number of galaxies per deg^2 per mag internal for $|b| > 25°$ (total area: ∼24000 deg^2). The J, H, and K_s source counts are represented with blue, green, and red lines, respectively. For comparison, the narrow (but deep) K-band galaxy counts of Glazebrook et al. (1994) and Gardner et al. (1997) are shown in black.

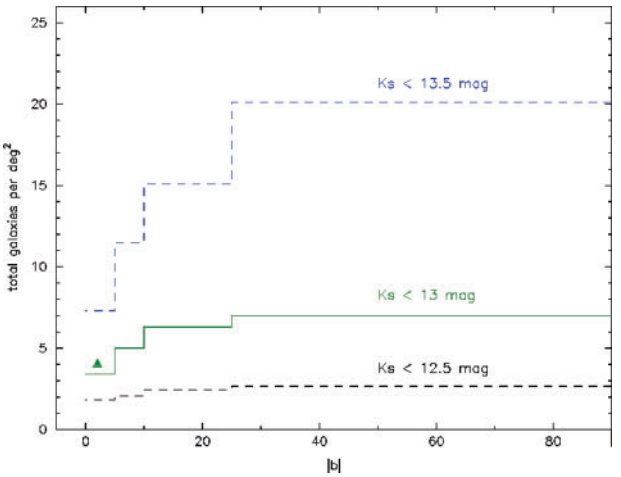

Figure 4 Cumulative number of galaxies per deg^2 with Galactic latitude. Three K_s-band flux limits are shown: 12.5 (black), 13.0 (green), and 13.5 mag (blue). All longitudes are used to draw the galaxy sample. For comparison, the integrated counts per deg^2 for a field deep in the ZoA ($l = 50°$, $b = 2°$) is indicated with a green triangle.

spirals (whose light is dominated by the younger, hotter disk population), dwarfs (low surface brightness) and compact objects (resolution limitations of 2MASS); see Jarrett (2000), Bell et al. (2003), and Jarrett et al. (2003). Consequently, the 2MASS galaxy catalog is partial to 'old' galaxies, which are typically lower in mass-to-light compared to gas-rich spiral galaxies (see also Rines et al. 2004 for a 2MASS study of the M/L ratio for clusters and inter-cluster regions).

3.2 Zone of Avoidance

A primary science driver of 2MASS was to penetrate the dust mask of the Milky Way. At near-infrared wavelengths, the opacity of dust is significantly smaller (∼1/10) compared to that of optical wavelengths, and thus amenable to probing observations. The Galactic 'zone of avoidance' (ZoA) is still, however, a formidable barrier due to the sheer number of stars that produce a foreground (confusion) 'noise'. Near the centre of the Milky Way the confusion noise is extreme, blocking nearly 100% of the background light; whereas far from the Galactic centre the confusion noise is minimal and the veil of the Milky Way is lifted at near-infrared wavelengths (see also Kraan-Korteweg & Jarrett 2004). As is shown in Figure 4, 2MASS penetrates deep into the ZoA away from the Galactic Centre, extracting galaxies well down to $|b| \sim 5°$, where detection completeness declines by ∼0.5 mag (Jarrett et al. 2000b).

3.3 All-Sky Galaxy Distribution

Simply by counting the number of galaxies along the line of sight it is a straightforward exercise to create a crude map of the local Universe. Spatial over-densities from galaxy clusters trace the large scale structure; see for example the beautiful maps of Courtois et al. (2004) who reconstructed the extragalactic sky using galaxies archived in LEDA. A more insightful way to map the surface density of galaxies is to integrate the 2-micron flux from all galaxies along the line of sight, thereby weighting the nearest structures and producing contrast between the Local Supercluster (cf. Tully 1982; Tonry et al. 2000) and the more distant 'cosmic web' structures; see Figure 5. This technique mitigates the biasing effects of non-uniform incompleteness due to surface brightness differences and galaxy morphology (see above). Figure 5 illustrates how 2MASS creates a uniform view of the local Universe, except for the extreme Galactic Centre, bridging the two hemispheres above and below the plane of the Milky Way (centre region of Figure).

A further enhancement to the all-sky maps is to colour-code the galaxies according to their total integrated flux. Since the integrated flux is strongly correlated with the distance to the object (assuming 2MASS galaxies have roughly the same luminosity; see the next Section), the colour-coding effectively adds depth to the surface density maps. In this way a qualitative view of the three-dimensional galaxy distribution is created, illustrated in Figure 6 using a Supergalactic projection. This simple and effective method delineates real large scale structure in the local Supercluster and beyond (Figure 6). We can marginally improve upon this 'photometric redshift' by correcting the luminosity estimate using the K-correction deduced from the near-infrared colours, described in the next Section.

4 The Local Universe

The current generation of large and uniform redshift surveys (e.g., CfA-RS, 2dF, SDSS, 6dFGS) provide a means to construct the three-dimensional space density of galaxies for volumes vastly exceeding those of the pioneering works from the 1980s. In the coming years new 'radial velocity machines', such as

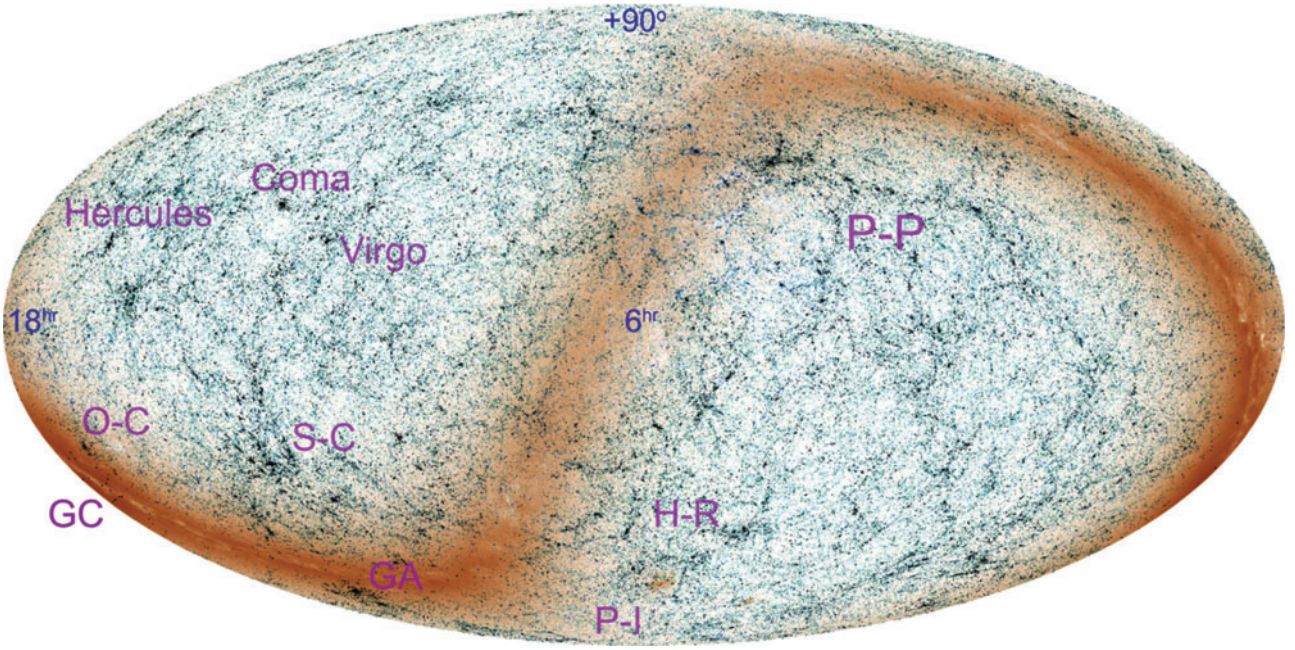

Figure 5 Equatorial view of the 2MASS galaxy catalog (6 h RA at centre). The grey-scale represents the total integrated flux along the line of sight — the nearest (and therefore brightest) galaxies produce a vivid contrast between the Local Supercluster (centre-left) and the more distant cosmic web. The dark band of the Milky Way clearly demonstrates where the galaxy catalog becomes incomplete due to source confusion. Some well known large-scale structures are indicated: P-P = Perseus–Pisces supercluster; H-R = Horologium–Reticulum supercluster; P-I = Pavo–Indus supercluster; GA = 'Great Attractor'; GC = Galactic Centre; S-C = Shapley Concentration; O-C = Ophiuchus Cluster; Virgo, Coma, and Hercules = Virgo, Coma, and Hercules superclusters. The Galactic 'anti-centre' is front and centre, with the Orion and Taurus Giant Molecular Clouds forming the dark circular band near the centre. See also Figure 1 for a Galactic projection of the local Universe.

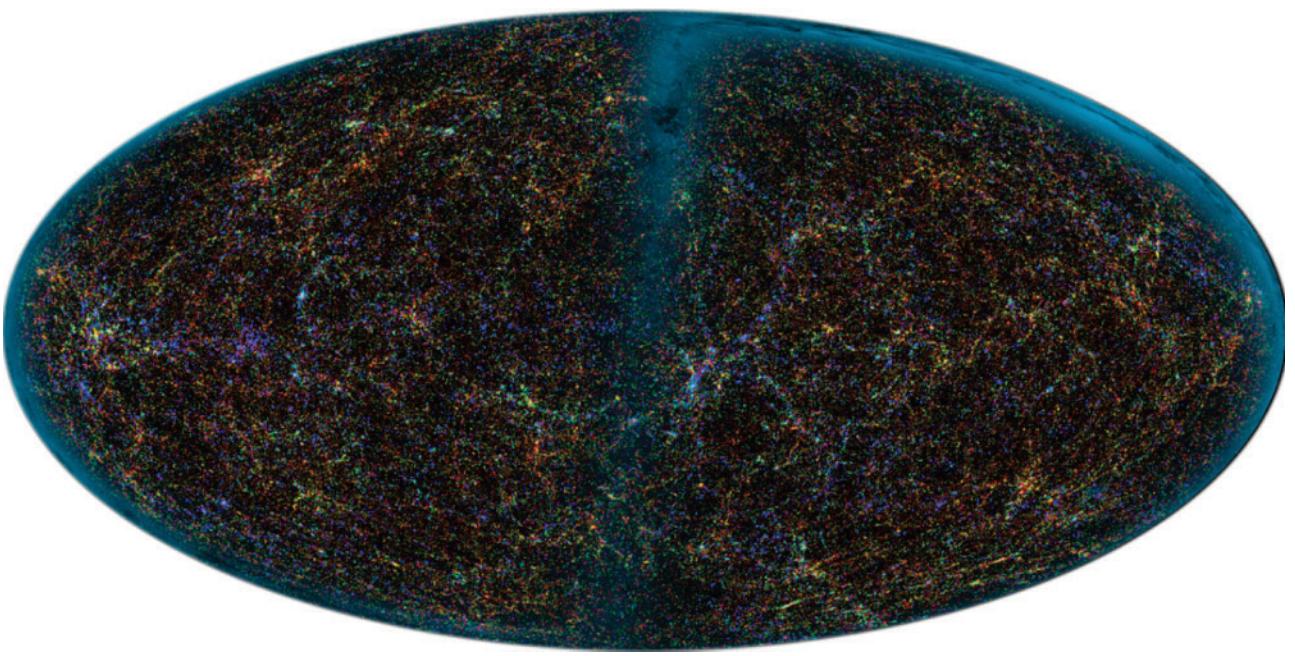

Figure 6 Supergalactic projection of the 2MASS galaxy catalog. Sources are RGB colour-coded according to their K_s-band integrated flux: brightest galaxies ($K_s < 10$) are blue, moderately bright galaxies ($10 < K_s < 12.5$) are green, and the faintest ($K_s > 12.5$) are red. The Local Supercluster as defined by de Vaucouleurs et al. (1976) extends along the equator crossing through the Virgo galaxy cluster (bright *blue* cluster, left-centre of image). The Milky Way is shown with a cyan colour scale, crossing the centre of the image and outer boundary. The Perseus–Pisces supercluster extends from the centre-right (northern Galactic hemisphere) down into the ZoA and out the other side to the southern Galactic hemisphere.

Echidna (Moore, Gillingham, & Saunders 2002), have the potential to increase redshift catalogs by an order of magnitude. Nonetheless, imaging surveys, including 2MASS, SWIRE, GOODS, and, in the coming years, WISE (Eisenhard & Wright 2003) catalog far more sources than the redshift surveys can ever handle. Velocity measurements will always be in the position of catching up with broad-band imaging. Meanwhile, broad-band photometric redshift techniques are improving as galaxy SEDs are expanded and refined to include the optical-NIR-MIR-FIR windows and different Hubble Types, driven by the large surveys from HST, SDSS, and Spitzer. A three-dimensional reconstruction of the local universe is therefore possible and within our reach using broad-band photometry from large-scale surveys. Here we use only the 2MASS galaxy catalog to create a first-look version of the local universe. With the coming of optical and mid-infrared broad-band and spectroscopy surveys, this view will sharpen and reach greater depths.

4.1 Photometric Redshifts

The three-band near-infrared photometry of 2MASS is used to estimate luminosity distances to galaxies. Although this technique is crude in terms of accuracy, it does provide a means to generate qualitative maps of the spatial distribution of galaxies and thereby construct an all-sky 'big picture' view of the local Universe. Here we adopt the technique devised by Kochanek et al. (2003). The fundamental assumptions of this method are that galaxies have roughly (1) the same luminosity and (2) their near-infrared colours are modified by cosmic reddening (Figure 7). The measured integrated flux is the primary component, while the near-infrared colours adds secondary information. This method is particularly adept at revealing galaxy clusters since the redshift uncertainty declines with the square root of the number of cluster members detected by 2MASS. We have determined that the photometric redshift of galaxy clusters is typically accurate to ∼20% using only 2MASS photometry.

By assuming that galaxies are standard candles, the distance or redshift is derived from the integrated flux, distance modulus, and luminosity distance. Here we correct for Galactic extinction and incorporate the cosmic reddening '*k*-correction', Figure 7, into the distance calculation for self-consistency between the measured colours and the inferred luminosity distance. Note that the scatter in the colour versus redshift (Figure 7) is large, comparable to the *k*-correction itself; hence, near-infrared colours alone are an insufficient discriminant of distance.

Independent studies of the K-band luminosity function (Cole et al. 2001; Kochanek et al. 2001; Bell et al. 2003) reveal consistent Schecter Function parameters (assuming $H_0 = 72\,\mathrm{km\,s^{-1}\,Mpc^{-1}}$): $M_\star = -24.0$ mag with a faint end slope index of about -0.8 to -1.0 (note that Bell et al. 2003 derive a slightly flatter slope than Kochanek et al. due to correction for incompleteness in the 2MASS XSC for low surface brightness galaxies). We adopt $M_\star$ as the standard candle for 2MASS galaxies. For the faintest 2MASS galaxies, $K = 14$ mag, the implied distance is 400 Mpc or $z \sim 0.1$. The actual distribution of K_s-band luminosity for all 2MASS galaxies with known redshifts is shown in Figure 8. The histogram peaks at -24.4 mag or so,

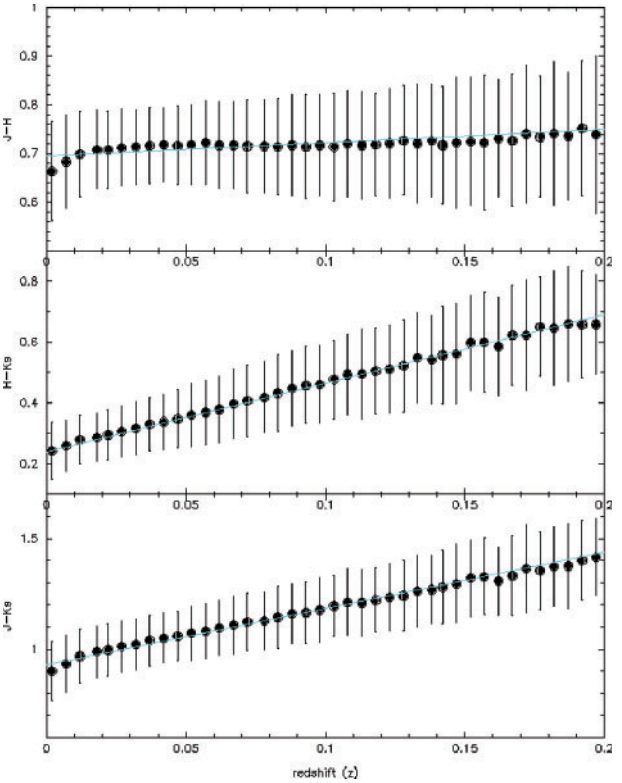

Figure 7 Galaxy near-infrared colours as a function of redshift. Cosmic reddening is the result of shifting of galaxy light from the H-band (1.6 μm) into the K_s-band (2.2 μm). The observed scatter (error bars) relative to the slope indicates that near-infrared colours alone are an inadequate discriminant of redshift.

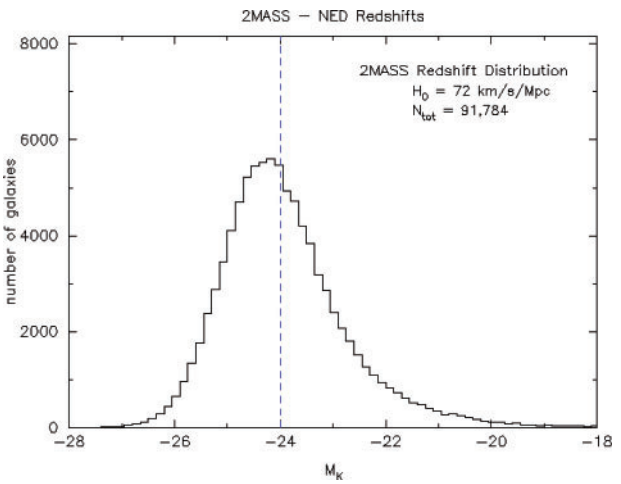

Figure 8 Luminosity distribution of 92000 2MASS galaxies as computed from redshift-derived distances. The redshifts were extracted from NED, the bulk of which come from the RC3, UGC, CfA, LCRS, 2dF, 6dFGS, and SDSS surveys. The faint end of the curve is subject to incompleteness due to the sensitivity limit of the redshift surveys.

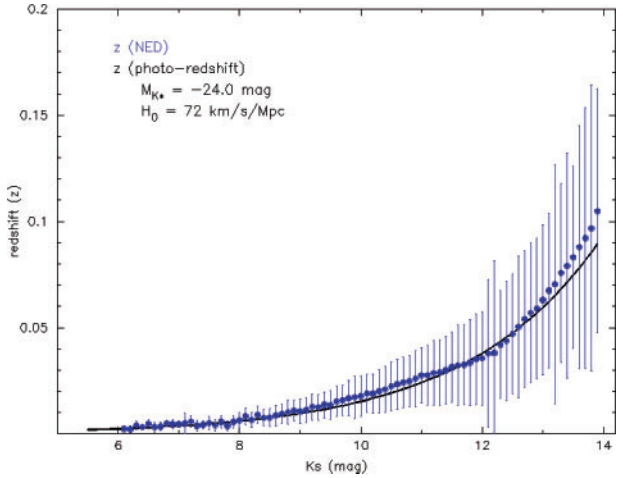

Figure 9 Redshift versus 2MASS K_s-band integrated flux. Photometric redshifts (black curve) are derived assuming $L_\star$ properties for 2MASS galaxies. These are compared to the radial-velocity redshifts (blue points). The error bars represent the scatter in redshift versus K_s-band integrated flux (i.e., ranging from luminous to sub-luminous galaxies). Note that the assumption that all galaxies have $L_\star$ luminosity works better for bright galaxies than for faint (low S/N) galaxies.

implying that 2MASS is sensitive to intrinsically luminous (early-type) galaxies. The fall-off in sources at the faint end is due in part to the sensitivity limit of redshift surveys. (Cautionary note: the 2MASS-NED redshift sample comes from a variety of surveys, each with their own biased selection effects — a prime motivation to carry out uniform and minimally biased redshift surveys, such as that of the 6dFGS.) Approximately 10^5 2MASS galaxies have radial velocity measurements, representing a small fraction (∼8%) of the total, but a significant fraction for the largest, nearby galaxies.

4.2 Results

A comparison of the photometric-derived redshifts with radial-velocity redshifts is shown in Figure 9, where we plot the redshift as a function of the K_s-band flux. The photometric redshifts appear to accurately predict the mean radial-velocity redshift per mag interval from the brightest (nearby) to the faintest (distant) galaxies. However, note the large scatter in the redshift distribution per mag interval — this is due to galaxies with intrinsically different luminosity — from the brightest ellipticals to the faintest dwarf galaxies. What this means is that 2MASS-only photometric redshifts provide the correct answer on average, but for any given galaxy the uncertainty is large, which is particularly severe for the faint end of the distribution.

And so we find that near-infrared photometric redshifts should provide an adequate, if qualitative, representation of the local Universe. Combining the 10^5 radial-velocity redshifts with the 10^6 photometric redshifts, a three-dimensional construct of the distribution of galaxies comprising the local Universe is created. Figure 1 represents a view into this three-dimensional construct. Here the 2MASS galaxies are projected onto a Galactic coordinate (equal-area) Aitoff grid with 3 arcmin pixels. Distance is denoted with colour coding, where blue represents the nearest galaxies ($z < 0.01$), green at moderate distances ($z \sim 0.03$), and red the most distant objects ($z > 0.06$). To enhance the contrast between the nearest clusters (e.g., Virgo) and the distant Universe, the pixel intensity is modified by the integrated flux along the line of sight (analogous to Figure 5). The effect is to brighten the colours of nearby galaxy clusters (e.g., the Virgo cluster appears blue-white in the Figure). Finally, the 2MASS point source catalog, representing the Milky Way, is incorporated into the projection. Near the galactic centre region (centre of image), the confusion noise completely swamps detection of background extragalactic objects.

4.3 The Cosmic Web

Figure 1 beautifully unveils the background extragalactic sky, separating the cosmic web from the obscuring foreground Milky Way. Galaxies are colour-coded by their inferred redshift (or distance from the Sun), thereby providing *depth* to the surface distribution of galaxies. Large-scale structures are clearly discerned, from the Local Supercluster (Virgo/Hydra/Centaurus) to the Perseus–Pisces (P-P) and Pavo–Indus (P-I) superclusters. (Figure 2 provides a key to the large-scale structures.) Probing orthogonal to this three-dimensional surface reveals the redshift distribution along the line of sight; an example is shown in Figure 10 for the Shapley Concentration (discussed below). The strong clustering seen at angular scales that span from arc-minutes (groups and clusters) to several degrees (super-clusters) confirms the result of Maller et al. (2003a) who measured the angular correlation function of galaxies in the 2MASS XSC, finding a slope of −0.76 with an amplitude of 0.11 at a 1° scale (out to 4°). Their results also indicate that higher surface brightness galaxies are clustered more strongly, consistent with the finding that early-type galaxies dominate massive clusters — the 'nodes' of the cosmic web.

As seen in Figure 1, a continuous chain of structures seems to wrap around Hydra/Virgo, up to Coma to the north, through Hercules to the east, down through P-P and around to P-I to the west, then extending up through the ZoA into the Shapley concentration. This is more easily seen when each redshift layer is shown separately; see Figure 11.

The Milky Way and Magellanic Clouds occupy the first ($z = 0$) redshift layer. The second layer ($z < 0.01$) is dominated by the Virgo, Fornax, and Hydra–Cen superclusters.

The third layer ($0.01 < z < 0.02$) is dominated by the P-P supercluster (left side of image) and the P-I superclusters, extending up into the ZoA and terminating as the Great Attractor region (i.e. Abell 3627) disappears behind a wall of Milky Way stars. An intriguing 'ring' or chain of galaxies seems to circle/extend from the northern to the southern Galactic hemisphere (see also Figure 1). It

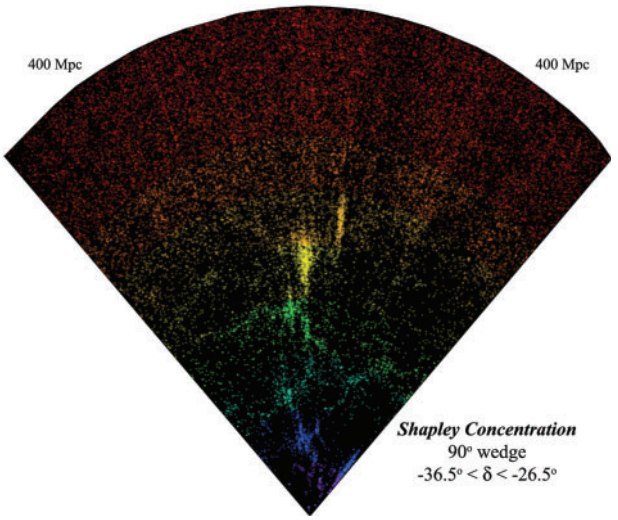

Figure 10 Redshift slice of the Shapley Concentration region, extending to the limit of the 2MASS galaxy catalog, $z \sim 0.1$ (400 Mpc). The equatorial RA slice is 90° between a declination boundary of $-36.5° < \mathrm{Dec} < -26.5°$. The points are colour-coded by redshift (see Figure 1). The 'finger of god' radial velocity artifacts trace galaxy clusters, including Abell 3558 (centre, yellow). The Hydra–Cen supercluster is foreground (blue fingers) to the Shapley Concentration.

is unknown whether this ring-like structure is physically associated with the cosmic web or an artifact of projection. The fourth layer ($0.02 < z < 0.03$) is characterised by compact galaxy clusters, including Coma (extreme top of image), Abell 3627 in the ZoA, the Ophiuchus cluster directly to the north of the Milky Way centre, and clusters associated with P-P. The 'Great Wall' of galaxies extends from Coma down towards Boötes and Hercules.

The fifth layer ($0.03 < z < 0.04$) is dominated by the Hercules supercluster (top, left of image), the 'Great Wall', Columba supercluster (bottom right of image), and the massive Shapley Concentration is beginning to appear. The sixth layer ($0.04 < z < 0.05$) showcases Abell 3558 of the enormous Shapley Concentration that lurks behind the nearby Hydra–Cen supercluster, and the Sculptor supercluster (bottom of image) makes its first appearance. The massive size and peculiar velocity field of the Shapley Concentration region suggests that it may be the most dominant 'attractor' in the local Universe; indeed the IRAS PSCz dipole (Rowan-Robinson et al. 2000) and 2MASS galaxy cluster dipole (Maller et al. 2003b) are located near this great structure.

The seventh layer ($0.05 < z < 0.06$) contains the backside of the Shapley Concentration, while the Sculptor supercluster dominates the southern hemisphere. The eighth and final layer ($z > 0.06$) contains the most distant structures that 2MASS resolves, including the Pisces–Cetus (located behind P-P), Boötes (located behind Hercules), Horologium, and Corona Borealis galaxy clusters. At these faint flux levels, the photometric redshifts are losing their ability to discern the cosmic web beyond 300 Mpc, smearing and degrading the resolution of the three-dimensional construct.

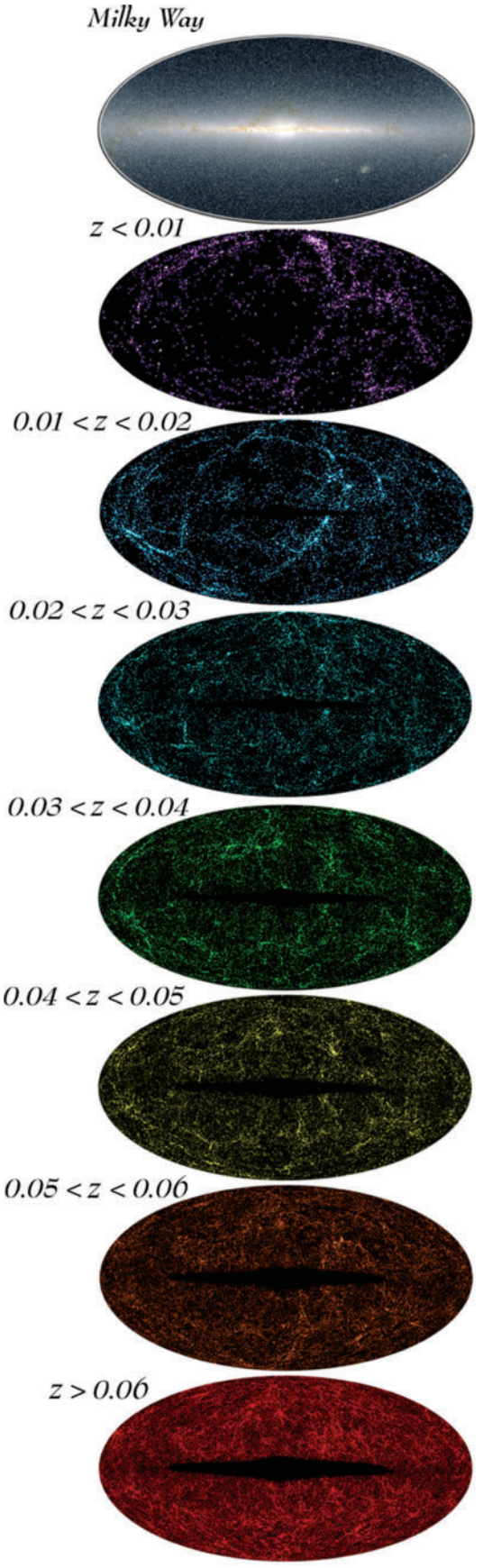

Figure 11 2MASS galaxy distribution separated by redshift layer. The colour scheme, when combined, creates the kaleidoscope panorama shown in Figure 1.

This is clearly demonstrated in Figure 10, where we show the redshift distribution for the Shapley Concentration region in a constant declination slice across the equatorial axis. The nearby galaxy clusters (Hydra–Cen) are easily discerned (note the radial-velocity 'fingers of god'), as are the rich galaxy clusters of Shapley (centre of image). Beyond $z > 0.06$, however, the distribution is smoothing out as the uncertainties in the photometric redshifts begin to dominate. But the intricate web of large scale structure extends well beyond this volume limit, as unmistakably demonstrated by the 2dF and SDSS galaxy surveys. With the addition of optical and mid-infrared photometry from future all-sky surveys (e.g., WISE), the photometric redshifts may be greatly improved, allowing reconstruction of the local Universe beyond 300 to 400 Mpc. Moreover, large redshift surveys (e.g., 6dFGS) will provide accurate distance estimates for large regions of the sky, further sharpening our view of the cosmic web.

4.4 Final Thoughts

The 2MASS catalog has proven to be quite versatile to the astronomical community: supporting observation and future mission planning, seeding studies of star formation and morphology in nearby galaxies, penetrating the zone of avoidance, providing the base catalog of redshift and Tully–Fisher HI surveys, and so on. But perhaps its most important function is to provide the 'big picture' context for analysis and interpretation of data concerning galaxy clusters, angular correlation and large scale structure, and the density of matter in the Universe. And so the primary motivation of this work, with the construction of qualitative 'road' maps to the local Universe, is to provide a broad framework for studying the physical connection between the local Universe (Milky Way, Local Group, Local Supercluster, 'Great Wall', etc.) and the distant Universe where galaxies and the cosmic web first formed. The best is yet to come.

Acknowledgments

The author would like to thank Joe Mazzarella (NED) and John Huchra (CfA) for kindly providing galaxy redshifts. Discussions with Roc Cutri, Mike Skrutskie, John Lucy, and Renee Kraan-Korteweg were very helpful. The referees of this paper are kindly thanked for their helpful suggestions. And special thanks to Joss Bland-Hawthorn for organising the LSS workshop (in honor of Brent Tully) that inspired this paper. This publication makes use of data products from 2MASS, which is a joint project of the University of Massachusetts and the Infrared Processing and Analysis Center, funded by the NASA and the NSF. This work was supported in part by the Jet Propulsion Laboratory, California Institute of Technology, under a contract with NASA.

References

Bell, E., McIntosh, D. H., Katz, N., & Weinberg, M. D. 2003, ApJS, 149, 289
Cole, S., et al. 2001, MNRAS, 326, 255
Courtois, H., Paturel, G., Sousbie, T., & Labini, F. 2004, A&A, in press
Cutri, R. M., et al. 2000, The 2MASS Explanatory Supplement (Los Angeles: 2MASS)
Eisenhardt, P., & Wright, E. 2003, Proc SPIE, vol. 4850, ed. J. C. Mather, 1050
Gardner, J. P., Sharples, M. R., Frenk, C. S., & Carrasco, B. E. 1997, ApJ, 480, L99
Glazebrook, K., Peacock, J. A., Collins, C. A., & Miller, L. 1994, MNRAS, 266, 65
Huchra, J., Davis, M., Latham, D., & Tonry, J. 1983, ApJS, 52, 89
Jarrett, T. H., Chester, T., Cutri, R., Schneider, S., & Huchra, J. 2003, AJ, 125, 525
Jarrett, T. H. 2000, PASP, 112, 1008
Jarrett, T. H., Chester, T., Cutri, R., Schneider, S., Skrutskie, M., & Huchra, J. 2000a, AJ, 119, 2498
Jarrett, T. H., Chester, T., Cutri, R., Schneider, S., Rosenberg, J., & Huchra, J. 2000b, AJ, 120, 298
Jones, D. H., et al. 2004, MNRAS, accepted
Karachentsev, I. D., Mitronova, S. N., Karachentseva, V. E., Kudrya, Yu., & Jarrett, T. H. 2002, A&A, 396, 431
Kochanek, C. S., White, M., Huchra, J., Macri, L., Jarrett, T. H., Schneider, S. E., & Mader, J. 2003, ApJ, 585, 161
Kochanek, C. S., et al. 2001, ApJ, 560, 566
Kraan-Korteweg, R., & Jarrett, T. H. 2004, ASP Conf. Ser. 'Nearby Large-Scale Structures and the Zone of Avoidance', eds. A. P. Fairall, & P. A. Woudt (San Francisco: ASP), in press
Lineweaver, C., Tenorio, L., Smoot, G., Keegstra, P., Banday, A., & Lubin, P. 1996, ApJ, 470, 38
Maller, A. H., McIntosh, D. H., Katz, N., & Weinberg, M. D. 2003a (astro-ph/0304005)
Maller, A. H., McIntosh, D. H., Katz, N., & Weinberg, M. D. 2003b, ApJ, 598, L1
Moore, A., Gillingham, P., & Saunders, W. 2002, ASP Conf. Ser. vol. 280, 'Next Generation Wide-Field Multi-Object Spectroscopy', eds. M. J. I. Brown, & A. Dey (San Francisco: ASP), 109
Rines, K., Geller, M. J., Diaferio, A., Kurtz, M., & Jarrett, T. H. 2004, AJ, 128, 1078
Rowan-Robinson, M., et al. 2000, MNRAS, 314, 375
Skrutskie, M., et al. 1997, in The Impact of Large-Scale Near-IR Sky Surveys, eds. F. Garzon et al. (Dordrecht: Kluwer), 25
Tonry, J. L., Blakeslee, J. P., Ajhar, E. A., & Dressler, A. 2000, ApJ, 530, 625
Tully, R. 1982, ApJ, 257, 389
Watson, F., et al. 2001, ASP Conf. Ser. vol. 232, 'The New Era of Wide Field Astronomy', eds. R. Clowes, A. Adamson, & G. Bromage (San Francisco: ASP), 421